

Characterization of Plasma-Irradiated SiO₂/Si Interface Properties by Photoinduced-Carrier Microwave Absorption Method

Masahiko Hasumi*, Jun Takenezawa, Tomokazu Nagao, and Toshiyuki Sameshima

Tokyo University of Agriculture and Technology, 2-24-16 Nakacho, Koganei, Tokyo 184-8588, Japan

Received July 9, 2010; accepted August 30, 2010; published online March 22, 2011

We report photoinduced carrier recombination induced by 13.56 MHz radio frequency argon plasma treatment for samples of silicon substrates coated with thermally grown SiO₂ layers. The transmissivity of a 9.35 GHz microwave was measured and analyzed under illumination of 532 nm green light to the top or rear surface. Irradiation of argon plasma at 100 W for 5 min caused substantial carrier recombination. The recombination velocity of the plasma-irradiated surface was estimated to be 6000 cm/s. Investigation of 100 kHz capacitance response characteristics as a function of bias voltage for metal oxide p-type silicon structures revealed that irradiation of argon plasma increased the fixed charge density from 3.2×10^{11} to 3.0×10^{12} cm⁻². Those changes were restored completely by heat treatment at 300 °C in air for 60 min.

© 2011 The Japan Society of Applied Physics

1. Introduction

Plasma processing is widely used for semiconductor device manufacturing.¹⁾ Plasma-induced damage has been studied extensively.²⁻⁴⁾ In general, plasma-induced damage is classified into the following three categories. Physical damage is primarily induced by high-energy ion bombardment during etching and surface modification.⁵⁾ Electrical damage is mainly related to the RF electric field, nonuniform plasma, nonuniform bias voltage, and electron-shading effect.⁶⁾ Radiation damage is induced by vacuum ultraviolet photons generated in the plasma. In particular, vacuum ultraviolet photons deeply penetrate the device⁷⁾ and produce many positive charges at or near the SiO₂/Si interface, lowering the device quality.^{8,9)}

The density of photoinduced carriers strongly depends on the carrier recombination properties at the surfaces and in the bulk semiconductor. Defects induce carrier recombination and reduce the density of photoinduced carriers. Measurements of microwave photoconductive decay (μ -PCD)¹⁰⁾ and quasi-steady-state photoconductance (QSSPC)¹¹⁾ have been widely used for the measurement of the photoinduced minority carrier lifetime. We have also developed a microwave free carrier absorption measurement system for nondestructive and noncontact investigation of photoinduced carrier properties.¹²⁻¹⁴⁾ The free carrier absorption effect is sensitive in the microwave frequency region. Free carriers in semiconductors respond to the incident electrical field of a microwave on the order of GHz and complex refractive indexes can be changed so that the transmissivity changes with the density of free carriers. When light is illuminated to a semiconductor sample, the change in microwave transmittance gives precise information of photoinduced carriers.

In this paper, we report a precise analysis of photoinduced carrier recombination properties induced by radio frequency argon plasma treatment for samples of silicon substrates coated with thermally grown SiO₂ layers using the free carrier microwave absorption method. We discuss changes in the effective minority carrier lifetime and surface recombination velocities at steps of plasma irradiation and heat treatment. We also investigate the 100 kHz capacitance response characteristics as a function of bias voltage ($C-V$)

for metal-oxide-p-type silicon (MOS) structures in the case of argon plasma irradiation.

2. Experimental Procedure

P-type silicon substrates with a resistivity of 8.3 Ω cm and a thickness of 525 μ m were prepared. Both surfaces were coated with 108-nm-thick thermally grown SiO₂ layers. 13.56 MHz radio frequency (RF) argon plasma was irradiated to the top surface of samples for 5 min by using a conventional capacitance coupled plasma treatment system as shown in Fig. 1. The RF power was 100 W and the substrates were kept at room temperature.

Photoinduced free carrier absorption was measured using a 9.35 GHz microwave transmittance measurement system constructed of waveguide tubes, as shown in Fig. 2. It had a narrow gap for measurement of the transmittance of sample wafers. A thin light illumination plate was also inserted facing the samples. Laser light at 532 nm was introduced using optical fibers to the light illumination plate, which gave uniform illumination to the samples. The light intensity was controlled from 0 to 19.3 mW/cm² at the surface of the sample by using optical filters. The intensity of the microwave transmitted through the samples was measured using an Agilent U2000 power sensor. The transmissivity at 9.35 GHz during light illumination to the top or rear surface was measured for samples before plasma irradiation, as-plasma-irradiated, and after heat treatment at 200 and 300 °C in air for 60 min. A finite element numerical calculation program including a Fresnel optical interference effect induced by the in-depth change in refractive index owing to photoinduced free carrier diffusion was used to estimate the density of free carriers from the experimental transmissivity.^{15,16)}

Both the top and rear SiO₂ layers for the argon plasma-irradiated sample were partially etched by 5% hydrofluoric acid for 30, 60, 120, 220, and 300 s to remove the physically damaged layers. The SiO₂ layer for the initial sample was also etched for comparison. The microwave transmissivity during light illumination to the top or rear surface was measured at each step of etching. The thickness of the remaining top SiO₂ layer was estimated by curve fitting of the calculated reflectivity spectra of ultraviolet and visible range to the experimentally obtained spectra.

After the argon plasma irradiation, the rear SiO₂ layer was removed by 5% hydrofluoric acid and MOS structures

*E-mail address: mhasumi@cc.tuat.ac.jp

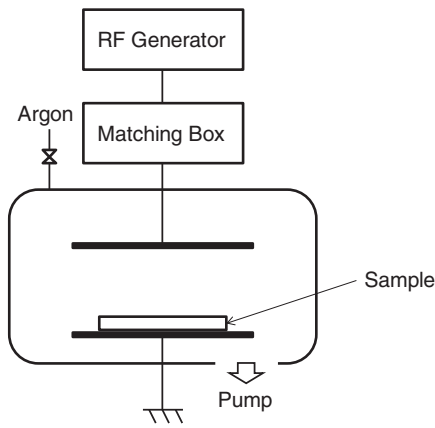


Fig. 1. Schematic apparatus of capacitance coupled RF argon plasma treatment system.

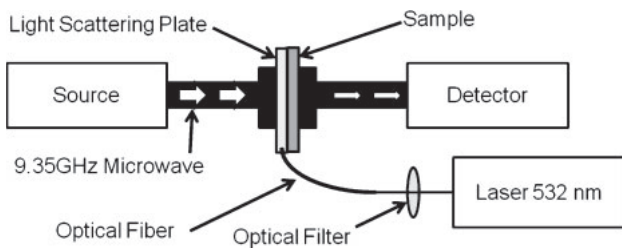


Fig. 2. Schematic apparatus of photoinduced carrier microwave absorption measurement system.

were formed by vacuum evaporation of aluminum to both the surfaces. The area of the top surface electrode was $1 \times 1 \text{ mm}^2$. The C - V characteristics for the initial, as-argon-plasma-irradiated, and heat-treated at 300°C in air for 60 min samples were measured using a conventional impedance analyzer with a frequency of 100 kHz. The densities of interface traps and fixed oxide charges were experimentally measured. The C - V characteristics under light illumination were also measured to investigate the properties of photoinduced carriers. A light-emitting diode array with a wavelength of 590 nm at an intensity of 24.0 mW/cm^2 was used for the light illumination source.

3. Results and Discussion

Figure 3 shows the changes in 9.35 GHz microwave transmissivity as a function of 532 nm light intensity illuminated to the top surface (square marks) and rear surface (circle marks) for the initial (open marks) and argon-plasma-irradiated (solid marks) samples. The initial sample showed decreases in transmissivity from 13.0 to 11.2% for light illumination at 19.3 mW/cm^2 to the top and rear surfaces. This means that the silicon surfaces were well passivated by thermally grown SiO_2 and a high density of photoinduced carriers existed under the illumination. On the other hand, no decrease in transmissivity was observed in the case of light illumination to the top surface for the argon-plasma-irradiated sample. Transmissivity slightly decreased from 13.2 to 12.4% in the case of the argon-plasma-irradiated sample for light illumination at 19.3 mW/cm^2 to

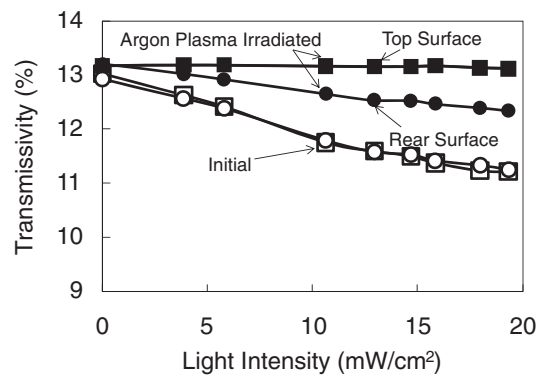


Fig. 3. Microwave transmissivity as a function of 532 nm light intensity illuminated to the top surface (square marks) and rear surface (circle marks) for the initial (open marks) and argon-plasma-irradiated (solid marks) samples.

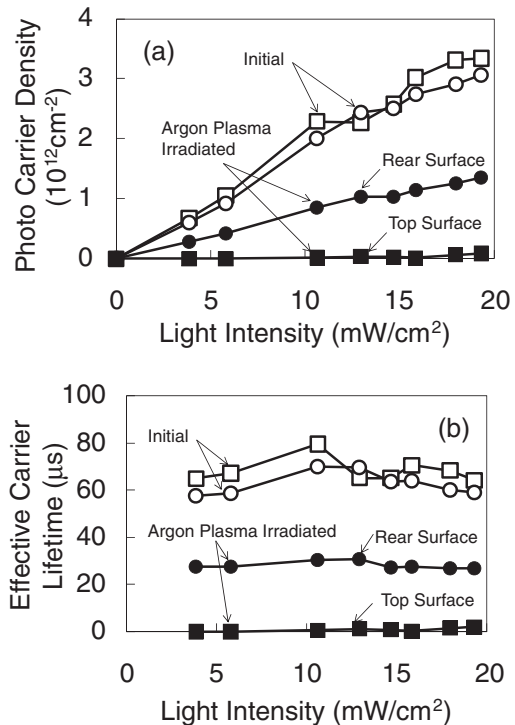


Fig. 4. Density of photoinduced minority carriers per unit area (a) and effective minority carrier lifetime (b) analyzed from the results of Fig. 1 as a function of the intensity of 532 nm light illumination.

the rear surface. Those results show that argon plasma irradiation caused substantial defects associated with serious carrier recombination in silicon.

Figure 4 shows the density of photoinduced minority carriers per unit area (a) and the effective minority carrier lifetime (b) as a function of the intensity of 532 nm light illumination obtained from the results of Fig. 3. The density of photoinduced minority carriers increased as the intensity of light illumination increased for the initial sample. The sample had the highest photoinduced carrier density of $3.3 \times 10^{12} \text{ cm}^{-2}$ at 19.3 mW/cm^2 . On the other hand, almost no photoinduced carriers were generated for the case of the top-surface-illuminated argon-plasma-irradiated sample.

The rear-surface-illuminated argon-plasma-irradiated sample showed the generation of photoinduced carriers, although the density was lower than that of the initial sample.

The photoinduced minority carrier density per unit area n shown in Fig. 4(a) directly gives the effective minority carrier lifetime τ_{eff} as

$$\tau_{\text{eff}} = \frac{n}{\eta(1-r)G}, \quad (1)$$

where G is the photon flux per unit area, r is the optical reflectivity at 532 nm, and η is the quantum efficiency for photoinduced carrier generation, which is assumed as 1 in this investigation. The initial sample had the highest effective minority carrier lifetime ranging from 64 to 79 μs for the light intensity ranging from 3.9 to 19.3 mW/cm^2 , as shown in Fig. 4(b). On the other hand, the argon-plasma-irradiated sample with 532 nm light illuminated on the top surface had a low effective minority carrier lifetime of 2 μs , which was the detection limit of the present experimental accuracy. In the case of rear surface illumination to the argon-plasma-irradiated sample, the effective minority carrier lifetime ranged from 27 to 31 μs . The effective minority carrier lifetimes of the top and rear surface illuminations were different for the argon-plasma-irradiated sample, which indicated that the recombination velocity of the top surface was increased by the argon plasma irradiation.

The in-depth distribution of photoinduced carrier density was analyzed from the results of Fig. 4 using a numerical program with the minority bulk carrier lifetime τ_b and recombination velocities of the top surface S_1 and the rear surface S_2 . A finite element numerical calculation program including a Fresnel optical interference effect induced by the in-depth change in refractive index owing to photoinduced free carrier diffusion was constructed to estimate the surface recombination velocities. In the case of the initial sample, the transmissivity showed the same behavior for both the top and rear surface illuminations. We assumed that the recombination velocities of both surfaces were equal $S_1 = S_2$. τ_b was assumed to be long enough at 0.01 s for initial silicon coated with thermally grown SiO_2 . The minority carrier diffusion length L determined by τ_b and the diffusion coefficient D was estimated to be 6 mm, which was much larger than the thickness of the silicon substrate. In this case, carrier recombination at the surface region was dominant. Numerical calculation with $S_1 = S_2 = 400 \text{ cm/s}$ showed a good fitting of the experimental transmissivity for the initial sample. S_1 was increased by the argon plasma irradiation because the photoresponse of the transmissivity became lower than that of the initial sample. The recombination velocity of the top surface S_1 was estimated to be 6000 cm/s , if the recombination velocity of the rear surface S_2 and τ_b were not changed by the argon plasma irradiation.

Figure 5 shows the calculated in-depth distribution of photoinduced minority carrier densities for the samples with 532 nm light illumination at 19.3 mW/cm^2 . The depth was measured from the light illuminated surface. The photoinduced minority carrier density for the initial sample monotonically decreased from the top surface to the rear

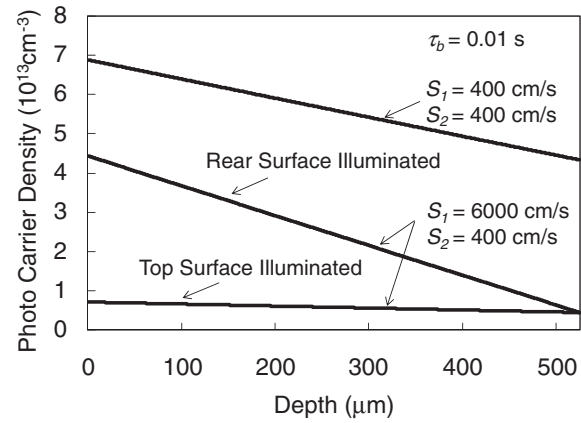


Fig. 5. Calculated in-depth distribution of photoinduced minority carrier densities for the samples with 532 nm light illumination at 19.3 mW/cm^2 . The depth of the light illuminated surface was defined as zero. The details of the surface recombination velocity S_1 , S_2 , and minority bulk carrier lifetime τ_b are provided in the text.

surface because the photoinduced carriers were generated at the top surface by light illumination. The minority carrier density becomes very low in the case that S_1 is very large, i.e., for the argon-plasma-irradiated sample with light illuminated to the top surface. On the other hand, a substantial carrier density can remain even if there is a surface with a high S_1 when light is illuminated to the other surface with a low carrier recombination velocity S_2 . This is because photoinduced carriers survive during travel across the silicon substrate until reaching the other surface.

The effective minority carrier lifetime τ_{eff} was determined by τ_b , S_1 , S_2 , D , and the thickness of the silicon wafer d . However, the relation was complicated by the carrier recombination and carrier diffusion properties.^{17,18} When surfaces are well passivated and surface recombination velocities are sufficiently low, a simple formula,

$$\frac{1}{\tau_{\text{eff}}} = \frac{1}{\tau_b} + \frac{S_1 + S_2}{d}, \quad (2)$$

is conventionally used to express the relation among τ_{eff} , τ_b , S_1 , and S_2 .¹⁹ τ_{eff} is independent of the carrier diffusion coefficient D . τ_{eff} is equivalent to τ_b when S_1 and S_2 are zero. τ_{eff} becomes low in the case of light illumination to the top surface if S_1 becomes very large. Especially in the case of a very long τ_b , τ_{eff} is approximately given as

$$\tau_{\text{eff}} = \frac{d}{S_1}. \quad (3)$$

In the case of rear surface illumination, a substantial carrier density can remain even if there is a surface with a high carrier recombination velocity S_1 . τ_{eff} in the case of rear surface illumination is higher than that in the case of top surface illumination. Therefore, we should take into account the photoinduced carrier diffusion in the silicon wafer in the case of unbalanced S_1 and S_2 . The carrier diffusion model gives τ_{eff} in the case of rear surface illumination with a very large S_1 and a very long τ_b as

$$\tau_{\text{eff}} = \frac{d^2}{2(D + S_2d)}. \quad (4)$$

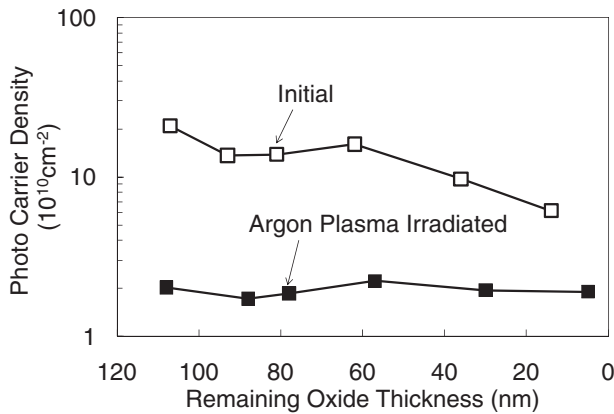


Fig. 6. Photoinduced carrier densities for the initial and argon-plasma-irradiated samples as a function of SiO₂ thickness. The light was illuminated to the top surface at an intensity of 1.1 mW/cm².

Detailed discussions have been reported separately.^{18,20)} According to the above analysis, we assume that the argon plasma irradiation induced the surface recombination sites but the silicon bulk was not damaged.

Next, we discuss the physical damage of the top surface caused by the argon plasma irradiation. After the 30 s etching by 5% hydrofluoric acid, the thickness of the top surface SiO₂ layer for the plasma-irradiated and initial samples decreased to 88 and 93 nm, respectively. The etching rate of the SiO₂ layer is high for the plasma-irradiated sample because of the plasma-induced physical damage. The difference in the top surface SiO₂ thickness between the argon-plasma-irradiated and initial samples was kept at approximately 5 nm in the case of an etching duration longer than 60 s. This result suggests that the physically damaged SiO₂ layer was less than 20 nm of the top region.

Figure 6 shows the photoinduced minority carrier densities per unit area for the initial and argon-plasma-irradiated samples with light illuminated at 1.1 mW/cm² to the top surface as a function of SiO₂ thickness. The photoinduced carrier density for the argon-plasma-irradiated sample was 2×10^{10} cm⁻² for the entire SiO₂ thickness range. It was lower than the density for the initial sample. If the physically damaged SiO₂ region affected the photoinduced carrier recombination properties, the photoinduced carrier density of the argon-plasma-irradiated sample showed the tendency to increase to that of the initial sample. However, the photoinduced carrier density of the argon-plasma-irradiated sample stays low after removal of the damaged region. This result suggests that the interface of SiO₂ and silicon was extensively damaged by the plasma irradiation.

Figure 7(a) shows the changes in microwave transmissivity as a function of 532 nm light intensity illuminated to the top surface for the as-plasma-irradiated sample and the samples heat-treated at 200 and 300 °C in air for 60 min. Heat treatment at 200 and 300 °C in air for 60 min resulted in marked decreases in the transmissivity of argon-plasma-irradiated samples from 13.2 to 11.6% and from 13.3 to 9.9%, respectively, with the light illumination at 19.3 mW/cm² to the top surface. The degree of transmissivity decrease for the sample with argon plasma irradiation followed by heat treatment at 300 °C was higher than that for

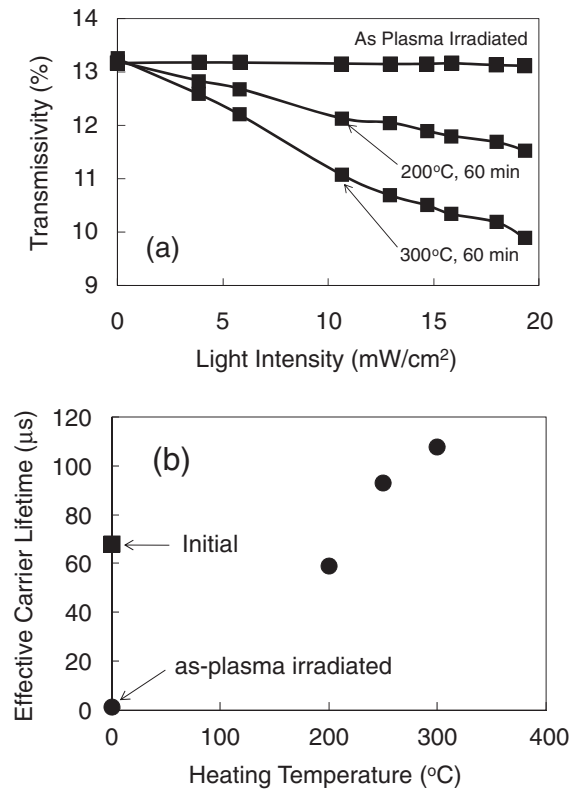


Fig. 7. (a) Microwave transmissivity as a function of 532 nm light intensity illuminated to the top surface for the as-plasma-irradiated sample and samples heat-treated at 200 and 300 °C in air for 60 min. (b) The changes in effective carrier lifetime by heat treatment for 60 min as a function of heating temperature. The effective carrier lifetimes for the initial and as-plasma-irradiated samples are also shown for comparison.

the initial sample, which indicates that heat treatment effectively decreased the defect states that the initial sample had as well as those caused by argon plasma treatment. Figure 7(b) shows the changes in effective carrier lifetime by heat treatment for 60 min as a function of heating temperature. The effective minority carrier lifetime increased as the heating temperature increased. The effective carrier lifetime for the sample heat-treated at 300 °C was 108 μs. Both S_1 and S_2 were decreased to be 200 cm/s by heat treatment at 300 °C for 60 min according to the analysis discussed above.

Figure 8 shows the $C-V$ characteristics for the initial sample (a) and the argon-plasma-irradiated sample (b) when they were measured in the dark field and under 590 nm light illumination at an intensity of 24.0 mW/cm². The $C-V$ characteristic in the dark field of the initial sample showed good electrical properties of the SiO₂/Si interface with densities of interface traps and fixed oxide charges of 3.4×10^{10} cm⁻² eV⁻¹ and 3.2×10^{11} cm⁻², respectively. On the other hand, it showed an increase in inversion capacitance under light illumination, as shown in Fig. 8(a). This increase clearly resulted from the diffusion current in depletion layers caused by photoinduced carriers. The photoinduced minority carriers generated surrounding Al electrodes effectively diffused into the depletion region underlying the Al electrodes because of the high diffusion length with a long effective lifetime given by low recombination velocity at the SiO₂/Si interface. The

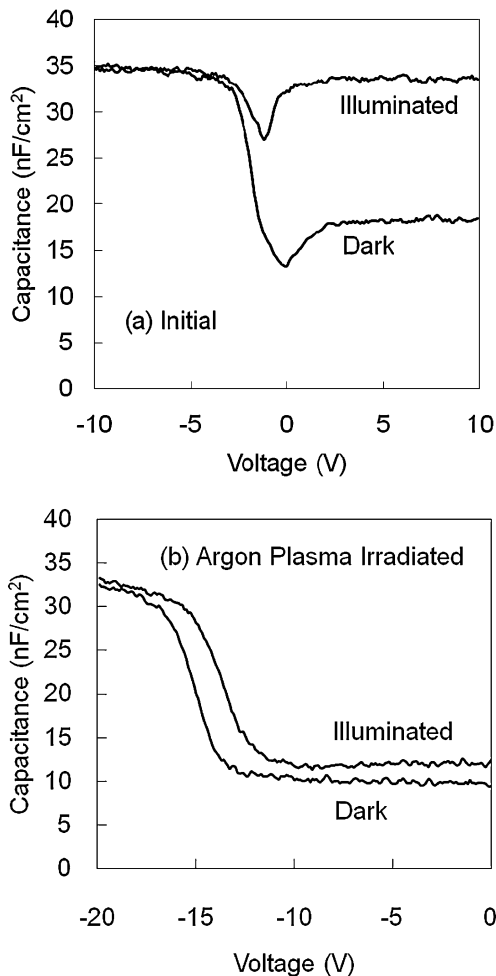


Fig. 8. Dark and photo illuminated 100 kHz C - V characteristics of initial (a) and argon-plasma-irradiated p-type MOS samples (b). Photo illumination was made by a 590 nm LED array at an intensity of 24.0 mW/cm².

depletion layer therefore became conductive and the inversion capacitance increased up to the oxide capacitance.

On the other hand, the flat band voltage was markedly shifted by 13.3 V in the negative direction by the argon plasma treatment. Irradiation of argon plasma increased the interface trap density to $6.6 \times 10^{11} \text{ cm}^{-2} \text{ eV}^{-1}$ and the fixed charge density to $3.0 \times 10^{12} \text{ cm}^{-2}$. Moreover, no marked increase in inversion capacitance under light illumination was observed in the case of argon plasma treatment, as shown in Fig. 8(b). The effective lifetime was decreased by argon plasma so that photoinduced carrier injection did not effectively occur into the inversion layer underlying Al electrodes. After the heat treatment at 300 °C for 60 min, the C - V characteristics in the dark field and under light illumination were restored to the characteristics that the initial sample had.

What increased the surface recombination velocity? We interpret that it was the vacuum-ultraviolet light in the argon plasma excited electron state of SiO₂ and/or silicon. It caused charge trapping states and built-in potential distribution at the SiO₂/Si interface, which caused an increase in the carrier recombination velocity. Therefore, the increase in the densities of the interface traps and fixed oxide charges were observed from the C - V characteristics.

4. Conclusions

We investigated the photoinduced carrier recombination properties for argon-plasma-irradiated SiO₂/Si structures. Argon plasma with an RF power of 100 W and a duration of 5 min was irradiated to 8.3 Ω cm p-type silicon coated with 100-nm-thick thermally grown SiO₂ layers. Irradiation of argon plasma caused substantial defects associated with serious carrier recombination in the SiO₂/Si interface region. The recombination velocity of the argon-plasma-irradiated surface was estimated to be 6000 cm/s, and that for the initial sample was 400 cm/s. We also investigated the C - V characteristics of argon-plasma-irradiated p-type MOS structures with a frequency of 100 kHz. Irradiation of argon plasma increased the fixed charge density from 3.2×10^{11} to $3.0 \times 10^{12} \text{ cm}^{-2}$. Decreases in effective lifetime and photoinduced carrier density by the argon plasma irradiation were also obtained using the C - V characteristics under light illumination. These defect states were restored completely by the heat treatment at 300 °C in air for 60 min.

Acknowledgement

This work was partially supported by a Grant-in-Aid for Science Research C (No. 22560292) from the Ministry of Education, Culture, Sports, Science and Technology of Japan.

- 1) H. Abe, M. Yoneda, and N. Fujiwara: *Jpn. J. Appl. Phys.* **47** (2008) 1435.
- 2) K. Eriguchi and K. Ono: *J. Phys. D* **41** (2008) 024002.
- 3) T. Yamada, K. Mizuno, K. Kitahara, and A. Moritani: *Jpn. J. Appl. Phys.* **44** (2005) 67.
- 4) K. Eriguchi, Y. Nakakubo, A. Matsuda, Y. Takao, and K. Ono: *Jpn. J. Appl. Phys.* **49** (2010) 056203.
- 5) N. Yabumoto, M. Oshima, O. Michikami, and S. Yoshii: *Jpn. J. Appl. Phys.* **20** (1981) 893.
- 6) K. Hashimoto: *Jpn. J. Appl. Phys.* **33** (1994) 6013.
- 7) J. A. R. Samson: *Techniques of Vacuum Ultraviolet Spectroscopy* (Wiley, New York, 1967) Chap. 1.
- 8) T. Yunogami, T. Mizutani, K. Suzuki, and S. Nishimatsu: *Jpn. J. Appl. Phys.* **28** (1989) 2172.
- 9) T. Yunogami, T. Mizutani, K. Tsujimoto, and K. Suzuki: *Jpn. J. Appl. Phys.* **29** (1990) 2269.
- 10) J. M. Borrego, R. J. Gutmann, N. Jensen, and O. Paz: *Solid-State Electron.* **30** (1987) 195.
- 11) G. S. Kousik, Z. G. Ling, and P. K. Ajmera: *J. Appl. Phys.* **72** (1992) 141.
- 12) T. Sameshima, H. Hayasaka, and T. Haba: *Jpn. J. Appl. Phys.* **48** (2009) 021204.
- 13) T. Sameshima, H. Hayasaka, and T. Haba: Proc. Workshop Active Matrix Flat Panel Displays, 2008, 205.
- 14) M. Hasumi, J. Takenezawa, Y. Kanda, T. Nagao, and T. Sameshima: Proc. 6th Thin Film Materials and Devices Meet., 2009, 100228114.
- 15) M. Born and E. Wolf: *Principles of Optics* (Pergamon, New York, 1974) Chaps. 1 and 13.
- 16) A. S. Grove: *Physics and Technology of Semiconductor Devices* (Wiley, New York, 1967) Chap. 5.
- 17) Y. Ogita: *J. Appl. Phys.* **79** (1996) 6954.
- 18) T. Sameshima, M. Shimokawa, J. Takenezawa, T. Nagao, M. Hasumi, S. Yoshidomi, N. Sano, and T. Mizuno: Proc. 6th Thin Film Materials and Devices Meet., 2009, 100228115.
- 19) J. W. Orton and P. Blood: *The Electrical Characterization of Semiconductors: Measurement of Minority Carrier Properties* (Academic Press, London, 1990) Chap. 4.
- 20) T. Sameshima, T. Nagao, S. Yoshidomi, K. Kogure, and M. Hasumi: *Jpn. J. Appl. Phys.* **50** (2011) 03CA02.